

NASA Technical Memorandum 103952

117774
P. 14

Thermal Degradation Study of Silicon Carbide Threads Developed for Advanced Flexible Thermal Protection Systems

Huy Kim Tran and Paul M. Sawko

(NASA-TM-103952) THERMAL
DEGRADATION STUDY OF SILICON
CARBIDE THREADS DEVELOPED FOR
ADVANCED FLEXIBLE THERMAL
PROTECTION SYSTEMS (NASA) 14 p

N92-32476

Unclass

G3/27 0117774

August 1992



Thermal Degradation Study of Silicon Carbide Threads Devel- oped for Advanced Flexible Thermal Protection Systems

Huy Kim Tran and Paul M. Sawko, Ames Research Center, Moffett Field, California

August 1992



National Aeronautics and
Space Administration

Ames Research Center
Moffett Field, California 94035-1000



Summary

Silicon carbide (SiC) fiber is a material that may be used in advanced thermal protection systems (TPS) for future aerospace vehicles. SiC fiber's mechanical properties depend greatly on the presence or absence of sizing and its microstructure. In this research, silicon dioxide is found to be present on the surface of the fiber. Electron Spectroscopy for Chemical Analysis (ESCA) and Scanning Electron Microscopy (SEM) show that a thin oxide layer (SiO_2) exists on the as-received fibers and the oxide thickness increases when the fibers are exposed to high temperature. ESCA also reveals no evidence of Si-C bonding on the fiber surface on both as-received and heat treated fibers. The silicon oxide layer is thought to signal the decomposition of SiC bonds and may be partially responsible for the degradation in the breaking strength observed at temperatures above 400°C . The variation in electrical resistivity of the fibers with increasing temperature indicates a transition to a higher band gap material at 350°C to 600°C . This is consistent with a decomposition of SiC involving silicon oxide formation.

Introduction

There is an increasing interest in the use of flexible ceramic blankets as TPS for atmospheric entry vehicles. The recent development of a silica blanket, Advanced Flexible Reusable Surface Insulation (AFRSI), for use as the TPS for specific locations on the space shuttle is one example (Goldstein, 1982; Trujillo, Meyer, and Sawko, 1984). Advanced flexible ceramic TPS needs to be fabricated from ceramic yarns and threads that can function in more severe thermal environments than silica blankets (Sawko, 1983).

Previous work has been done to characterize the mechanical properties of low and high boria content aluminoborosilicate threads. The results showed that, although both threads have high breaking strengths at temperatures below 1000°C , the strength of both dropped rapidly when exposed to temperatures above 1000°C (Sawko and Tran, 1987). Other studies have shown that SiC threads have high temperature strength (Sawko and Vasudev, 1989) and SiC fabrics exhibit promising optical properties over a wavelength range from 500 to 2500 nm (Covington and Sawko, 1986). It has been suggested that SiC thread be used in future flexible TPS development. In high temperature applications, the characterization of SiC thread is initiated and becomes important to ensure the efficient thermal performance.

Therefore, the objectives of this paper are to: (1) describe the mechanical behavior of SiC thread over a range of temperatures and to examine the influence of the thermal

and electrical properties, and (2) examine the microstructure of SiC fibers used in the construction of SiC threads and to determine the SiC fiber's microstructure effects on the breaking strength of the threads.

Symbols

AFRSI	Advanced Flexible Reusable Surface Insulation
ESCA	Electron Spectroscopy for Chemical Analysis
eV	Electron Volts
KOH	Potassium Hydroxide
KNO_3	Potassium Nitrate
r^*	Measured Resistance
SEM	Scanning Electron Microscopy
SiC	Silicon Carbide
SiO_2	Silicon Oxide
TGA	Thermogravimetric Analyzer
TPS	Thermal Protection Systems
XPS	X-ray Photon Spectroscopy
XRD	X-ray Diffraction
ρ	Resistivity
α	Thermal Expansion Coefficient

Experiment

Material

SiC filaments used to construct the threads in this study were supplied by Dow Corning. SiC filaments consist mostly of β -SiC structures and have a diameter of about 10 to 20 μm . To fabricate the thread, the filaments are bundled into a twistless SiC tow of 250 filaments. The tow is then twisted in the S-direction at 122 turns per meter, into a yarn of 900 denier (900 gm per 9000 m). The SiC thread is prepared by plying together two twisted yarn bundles to form a sewing thread containing a total of 500 round cross sections of continuous filaments. The yield count of this thread is listed as 200 tex (200gm/1000m), which corresponds to 1800 denier (1800 gm/9000m) or 2480 yards per pound. A 1.5% weight, P-type modified epoxy was applied to the yarn as a sizing lubricant that can be removed by heat cleaning at 400°C .

Test and Characterization Methodologies

Elevated temperature measurement of the break strength— The SiC thread breaking strengths was

determined using the computerized Instron Model 1211 and a custom built furnace that was used in the characterization of the aluminoborosilicate threads (Sawko and Tran, 1987).

A 76 cm thread specimen was mounted between custom holding clamps that provided the test sample's final gage length of 23 cm. Only 2.54 cm of the center section of the specimen was heated in the furnace. A load cycle function was also used to continuously impose a 0.11 kg load on the entire specimen to remove any excess looseness induced by the yarn twisting or by the thermal expansion of the thread itself. After a 10 min heat soak at a specified temperature, the specimen was pulled to failure and the break strength was obtained. Six specimens are tested at each temperature to determine the average break strength.

Electrical resistivity measurement— The electrical resistance (r^*) of SiC thread was measured by using a high impedance ohmmeter. The two electrical connectors were clamped to the two portions of the thread outside the furnace on the assumption that the heat transfer to the surrounding of the furnace was minimal. The ohmmeter's range was 0.001 $\mu\Omega$ to 1000 M Ω . The resistance values were obtained independently at each test temperature.

Thermal analysis— A Dupont 950 Thermogravimetric Analyzer (TGA) was used to determine the decomposition temperature of the organic sizing on the as-received thread. A 10 mg sample was pulverized and heated in air at a heating rate of 10°C per minute until the weight remains constant. This indicated the complete removal of any organic sizing.

Surface characterization— Electron Spectroscopy for Chemical Analysis (ESCA) was used to characterize the surface chemistry of previously heated SiC fibers. The ESCA technique provided both compositional and chemical bonding information within the outer 10 nm of any solid surface for all elements except hydrogen and helium.

Survey scans from 0 to 1000 electron volts (eV) were obtained from the surface of three fiber bundles to determine which elements were present. High resolution spectra were then acquired to help characterize the surface chemistry of the principal carbon, oxygen, and silicon peaks.

Microstructural characterization— SEM and x-ray diffraction (XRD) were also used to further determine the microstructure of the SiC fibers. To reveal the microstructural details in the fiber, a mixture of potassium hydroxide (KOH) and potassium nitrate (KNO₃) were used to etch the sample. The etchant was heated to 500°C and the fiber was etched for 20 sec to clean the surface and was then air dried.

Results and Discussion

The breaking strength of the as-received SiC thread as a result of temperature is shown in figure 1. The strength degradation exhibited by the thread when exposed to high temperatures can be divided into three characteristic regimes.

Regime I, shown in figure 1, occurs from 23°C (room temperature) to 350°C. The SiC thread's breaking strength was clearly not dependent on temperature. The as-received SiC thread had about 1.5% weight of modified P-type epoxy sizing, which was believed to be a partial contributor to the high initial and constant breaking strength values at this temperature range. The sizing probably reduced the friction of individual filaments rubbing on each other while under load. The TGA of the as-received SiC thread from 23°C to 700°C is shown in figure 2. The epoxy sizing was gradually removed at 250°C and totally decomposed at 400°C. The sizing applied to the SiC yarn during the twisting process acted as a lubricant and its strength as a film former was trivial compared to the overall breaking strength of the SiC thread seen in Regime I (fig. 1). Therefore, the major contribution to SiC thread breaking strength from 23°C to 350°C was the actual strength of the sized SiC fiber itself.

In Regime II, the major loss in SiC thread breaking strength occurred in a temperature range of 350°C to 600°C (fig. 1). This degradation was due both to sizing removal and the concurrent transition of SiC to SiO₂ on the fiber surface. However, the sizing effect appeared to contribute less compared to the latter effect. The surface transition of SiC to silicon dioxide was due to the SiC bond decomposition and the subsequent formation of Si-O. This transition was evident in the shift of the electrical resistivity measurements from a SiC dominant to a SiO₂ dominant effect. Figure 3 shows the logarithm of resistivity as a function of temperatures and is a classic Arrhenius-type relation (eq. (1)). The resistivity of SiO₂ and SiC, shown as curves 1 and 2 respectively in figure 3, were calculated by using data from literature (Massigoel, 1986) and the governing eq. (1). Curve 3 in figure 3 is the resistivity calculated by using the actual measurement of the SiC thread and eq. (2).

$$\rho = \rho_0 \exp(-E_A/RT) \quad (1)$$

$$\rho = \rho_0 + Ar^*/L \quad (2)$$

where

ρ is the resistivity in ohms-cm

ρ_0 is the resistivity at 25°C (Massigoel, 1986)

E_A is the activation energy of SiC

T is the temperature, °C
 R is the universal gas constant
 A is the cross section area of the thread, cm²
 L is the gage length of the heated area, cm
 r* is the measured resistance, Ohms

$$\alpha_{\text{SiC}} = 3 \times 10^{-6} / ^\circ\text{C}$$

$$\alpha_{\text{SiO}_2} = 5 \times 10^{-7} / ^\circ\text{C}$$

It was assumed that as the temperature increased, a minimal amount of heat was transferred to the portion of the fiber external to the furnace. The parallel nature of the SiO₂/SiC composite fiber resistance was ignored. The transition in electrical resistivity in figure 3 was consistent with SiC dominated behavior to SiO₂ dominated behavior. This behavior correlated with the transition in breaking strength observed in figure 1. The transition of SiC to SiO₂ was clearly shown by a large drop in resistivity between 400°C to 600°C. The intercept of curves 1 and 2 also represented the initial transition of SiC to SiO₂ at 350°C.

ESCA was performed to provide the compositional and chemical bonding information for all existing elements. The ESCA data obtained for the as-received fiber, 600°C fiber, and 1200°C fiber are shown in figures 4–6. High resolution C(1s), O(1s), and Si(2p) data are identified by the suffices "a" through "c," respectively (figs. 4–6).

Figures 4–6 show that the outer surfaces of three fibers are comprised almost entirely of silicon oxide (probably SiO₂). All three figures show a similar effect. The high intensity peak occurred at 532.5 eV showing a significant number of oxygen atoms on the fiber's surface. This observation was expected. It was, however, surprising that there was no evidence of Si-C bonding on the as-received fiber surface. If the Si-C bonding existed, it would have manifested itself in the Si (2p) high intensity spectrum by a peak at 101 eV and in the C(1s) high intensity spectrum with a peak at about 283 eV. However, previous work conducted to determine the surface chemistry of the as-manufactured Nicalon (SiC) fibers showed a molecular composition of SiC: 0.38SiO_{1.2}C_{0.4}:0.54C. This was determined from XPS (x-ray photon spectroscopy) analyses (Lahaye, Schreck, and Ehrburger, 1991). The Si (2p) peak at 103 eV and the O(1s) peak at 532.5 eV confirmed the presence of Si-O bonding. Therefore, it is rationalized that the high temperature treatment accelerated the Si-O bond formation and thickened the oxide layer causing the rapid SiC thread strength loss observed from 350°C to 600°C. This degradation was further enhanced by the mismatch in thermal expansion coefficients of SiC and SiO₂, which might significantly strain the interface between the fiber and oxide film. The respective coefficients are shown below (Handbook of Chemistry and Physics, 1980-81):

In Regime III (fig. 1), a gradual decrease in breaking strength occurred over a temperature range of 600°C to 1200°C. Figure 7 shows the expanded spectrum of the sample fiber heated at 1200°C to better illustrate the binding energy data. It is evident that Si(2p) and O(s) are dominant at 103.5 eV and 532.5 eV. This confirms the rapid thermal growth process of the oxide layer on the SiC fiber surface at a high temperature. A change in color from black to greenish-black to blue-black was observed on the fiber surface at 1000°C and 1200°C. This phenomenon represented the rapid growth of the silicon oxide layer on the fiber surface. Using the silicon oxide color chart in Massigoel (1987), the layer thickness was estimated to be about 160 nm to 280 nm. The thermal growth process of the oxide layer caused the continuous and gradual degradation in breaking strength at temperatures above 600°C. In addition, oxidation of free carbon at temperatures above 800°C occurred leaving surface pits on the fibers, which further lowered the strength of the fibers.

XRD analysis was also used to investigate the changes in crystal structure that might contribute to the continuing drop in breaking strength observed in figure 1. Both the as-received and 1200°C fibers were analyzed using copper K radiation at a rate of 2 degrees per minute from 10° to 60°. Shown in figures 8 and 9 are the crystal structure of both the as-received and heat treated fiber. There was no significant change in microstructure or the volume fraction of the second phase observed. The peak at 33° was due to the amorphous or β-SiC structure that constituted the main volume fraction of the subject fibers.

Additional information to support the proposed explanation for the SiC fiber in breaking strength degradation was the phase diagram of Si-C shown in figure 10 (Olesinski, 1984). There are free silicon atoms in the silicon carbide material if it is manufactured in an environment below 1300°C. These free Si atoms can act as impurities and/or interstitial atoms in the SiC structure and promote the formation of Si-O bond when the material is exposed to an oxygen rich environment. Finally, SEM revealed the presence of SiO₂ film on the as-received fiber surface (fig. 11(a)) and a thicker oxide layer at 1200°C (fig. 11(b)). Subsequently, as the SiO₂ layer grew thicker, its mechanical strength became dominant at high temperatures. It devitrified (crystallized) to form cristobalite, which is the metastable form of SiO₂ (the lowest energy state of the silica system). This devitrification process, along with the mismatch in the thermal expansion coefficients of SiO₂ and SiC, was another reason for the loss in breaking strength of SiC shown in Regime III (fig. 1).

Conclusions

The effect of temperature on the breaking strength of SiC threads can be divided into three regimes. Regime I showed sizing was used only to lubricate and protect the thread yarns during manufacturing and had no negative effect on the mechanical strength of SiC threads. Regime II associated degradation with the thermal growth process of oxide layer formation and the transition of SiC to SiO₂ on the fiber surface. ESCA confirmed the presence of an oxide layer on the as-received fiber surface as well as on those exposed to temperatures between 600°C and 1200°C. This oxide layer grew more rapidly at higher temperatures. A greenish-black to blue-black color transition was observed as the temperature increased from 1000°C to 1200°C, indicating the oxide layer thickness was approximately 200 nm. ESCA also showed no evidence of Si-C bonding on either the as-received or heat treated fibers' surfaces. This may be in contrast to previous work conducted to determine the surface chemistry of the as-manufactured Nicalon SiC fibers. The lack of Si-C bonding was probably caused by the dissociation of the bond and the formation of Si-O bonds. This transition is further supported by the change in resistivity measurement (SiC dominant to SiO₂ dominant behavior). XRD analysis also confirmed no crystal structure changes from 23°C to 1200°C and there was a broad peak at 33° Bragg angle, which indicated the SiC retained its amorphous or β-SiC structure during the heat treatment. Therefore, the major contribution to the loss in breaking strength of SiC threads was the presence of the oxide layer, which is further enhanced by the transition of Si-C to Si-O bonds.

References

- Covington, A. E.; and Sawko, P. M.: Optical Properties of Advanced Ceramic Fabrics. AIAA Paper 85-2274, 1986.
- Goldstein, H. E.: Fibrous Ceramic Insulation. NASA CP-2252, 1982, pp. 261-275.
- Handbook of Chemistry and Physics, 61st ed. CRC Press, 1980-1981.
- Lahaye, J.; Schreck, P.; and Ehrburger, P.: XPS Analysis of Silicon Carbide Based Fibers. Extended Abstract, 20th Biennial Carbon Conference, U.C. Santa Barbara, Calif., 1991, p. 244.
- Massigoel: Handbook of Thin Film Technology, 1986.
- Olesinski, R. W.; and Abbaschian, G. J.: The C-Si System. Bulletin Alloy Phase Diagrams, 1984, vol. 5, no. 5, pp. 486-489.
- Sawko, P. M.: Flexible Thermal Protection Materials. NASA CP-2315, 1983, pp. 179-192.
- Sawko, P. M.; and Tran, H. K.: Influence of Thread Construction on Strength of Ceramic Sewing Threads. SAMPE Quarterly, vol. 18, no. 4, 1987, pp. 32-39.
- Sawko, P. M.; and Vasudev, A.: Development of a Silicon Carbide Sewing Thread. SAMPE Quarterly, vol. 20, no. 4, 1989.
- Trujillo, B. M.; Meyer, R. M., Jr.; and Sawko, P. M.: In-flight Load Testing of Advanced Shuttle Thermal Protection Systems. AIAA Paper 83-2704, 1984.

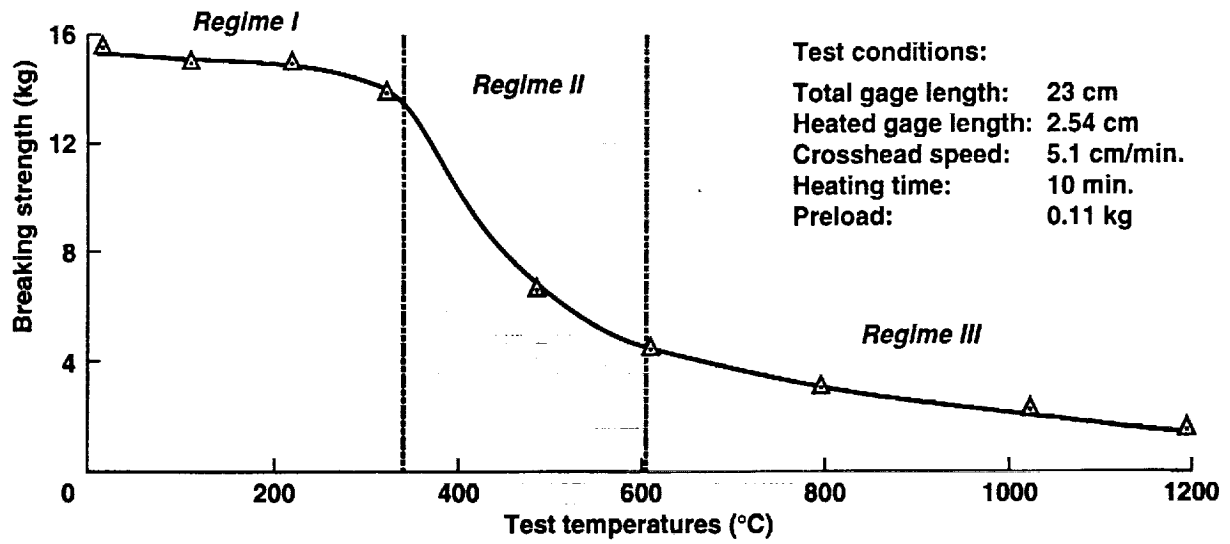


Figure 1. Effect of sizing and temperature on breaking strength of SiC threads.

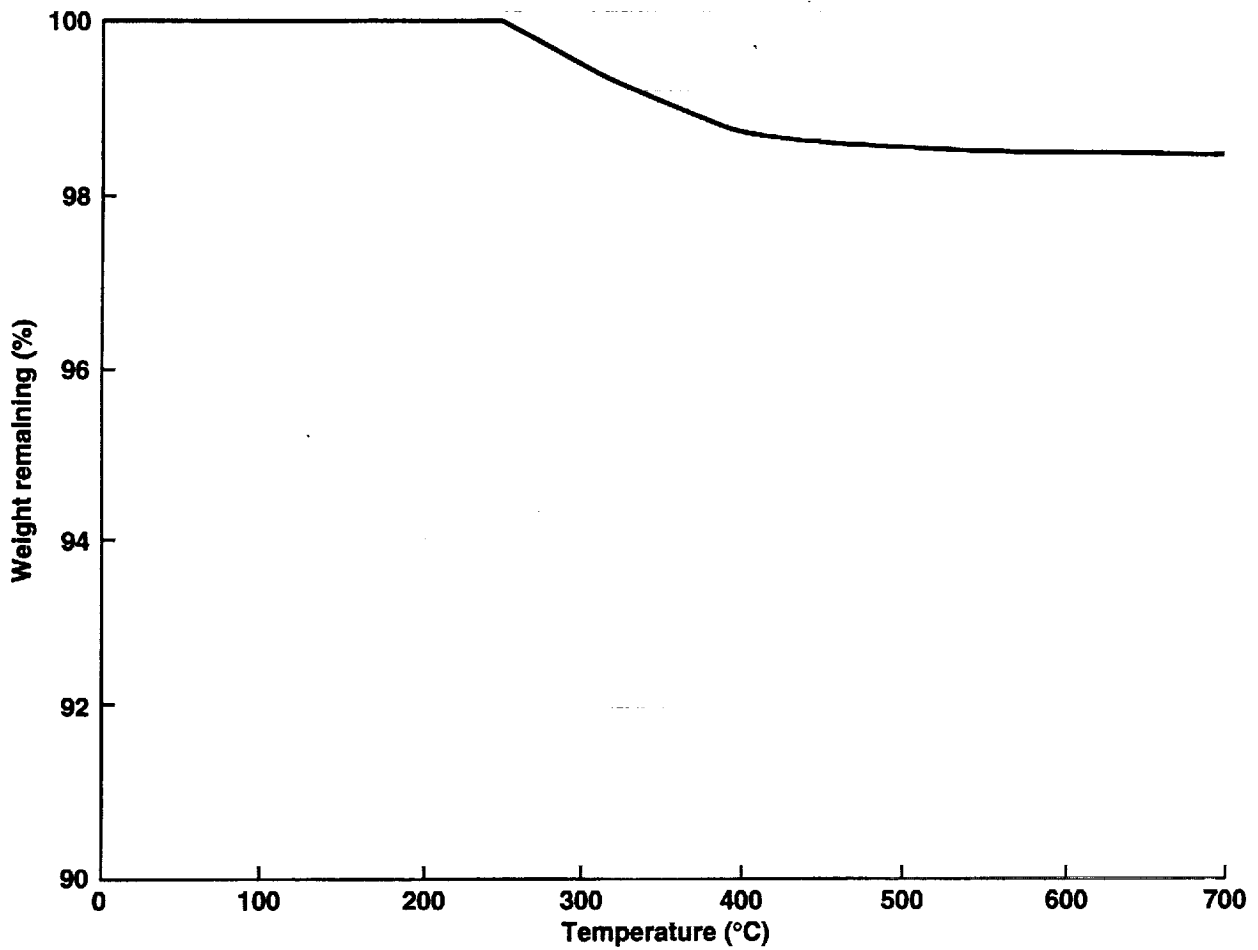


Figure 2. Thermogravimetric analysis of SiC thread.

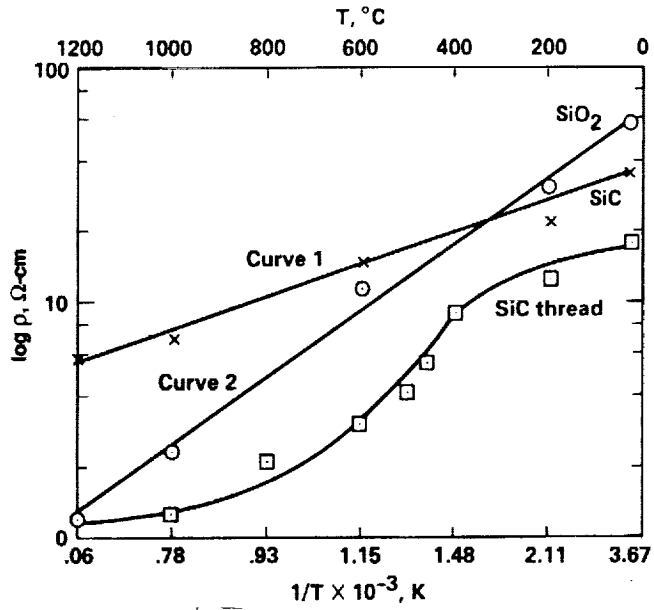


Figure 3. $\text{SiC} \rightarrow \text{SiO}_2 \rightarrow$ perhaps high temperature doped extrinsic behavior.

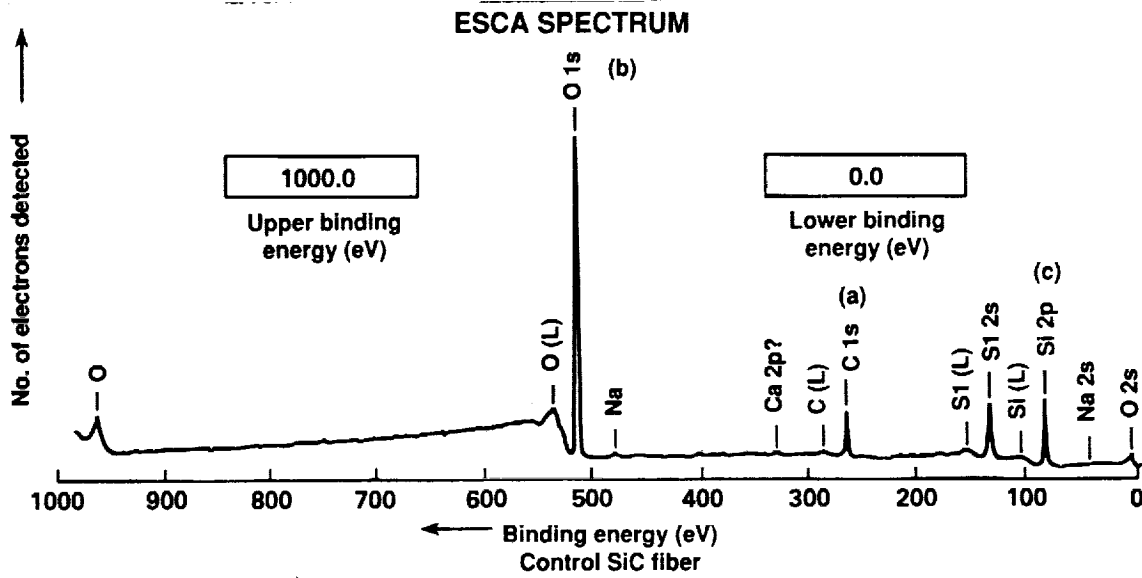


Figure 4. ESCA spectrum of as-received SiC fiber.

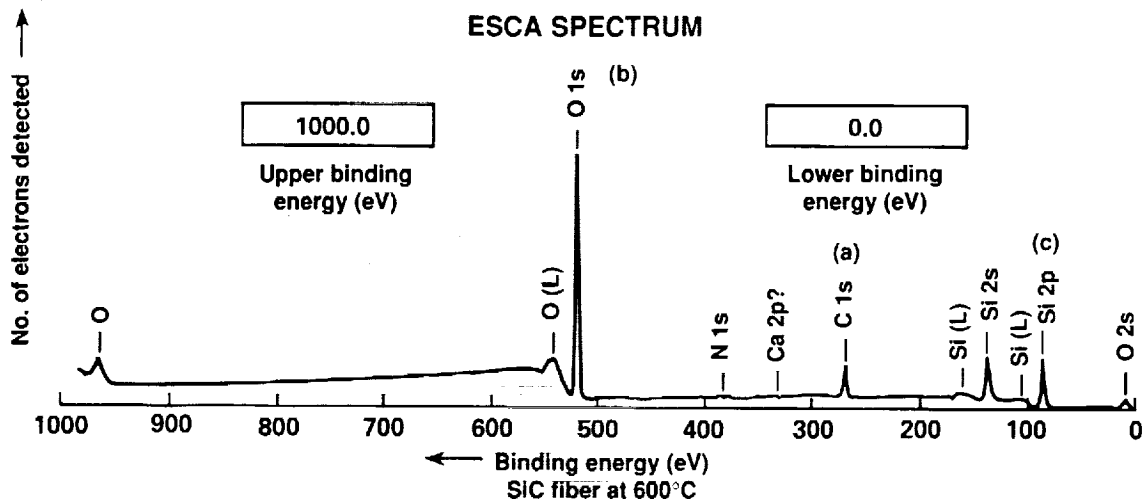


Figure 5. ESCA spectrum of SiC fiber exposed at 600°C for 10 min.

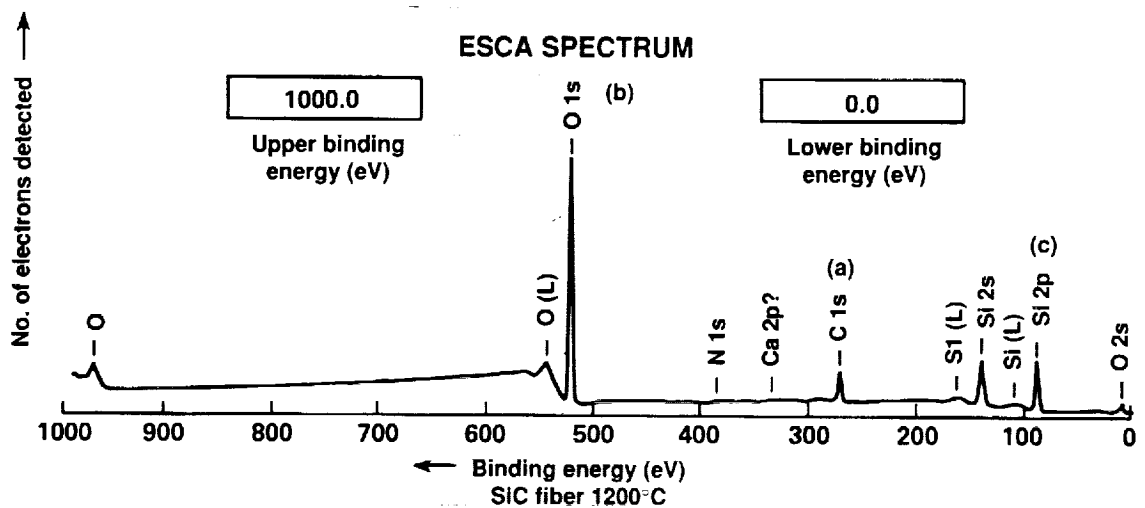


Figure 6. ESCA spectrum of SiC fiber exposed at 1200°C for 10 min.

ESCA SPECTRUM

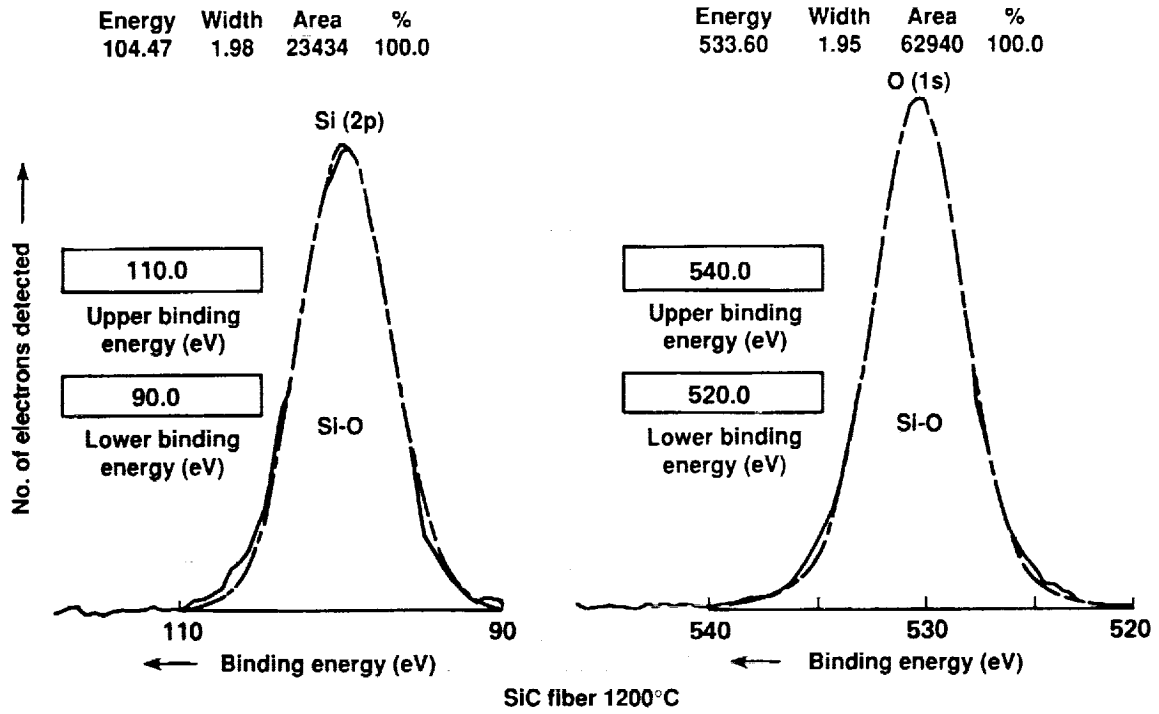


Figure 7. Expanded ESCA spectrum on Si-O region of SiC fiber.

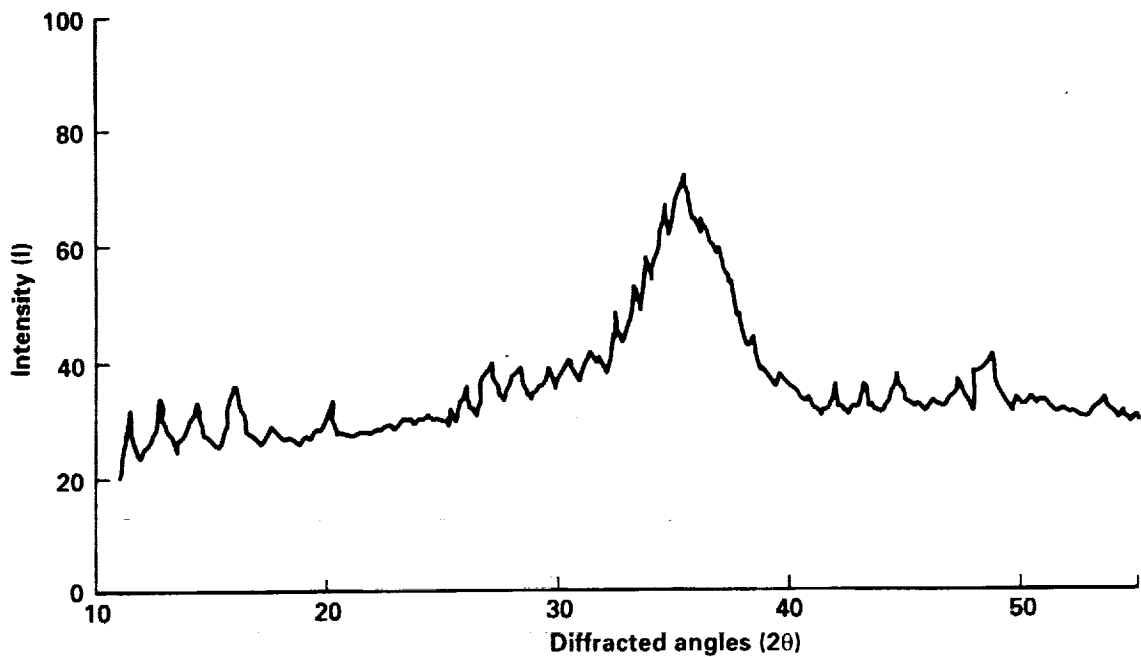


Figure 8. X-ray diffraction analysis of as-received SiC fiber.

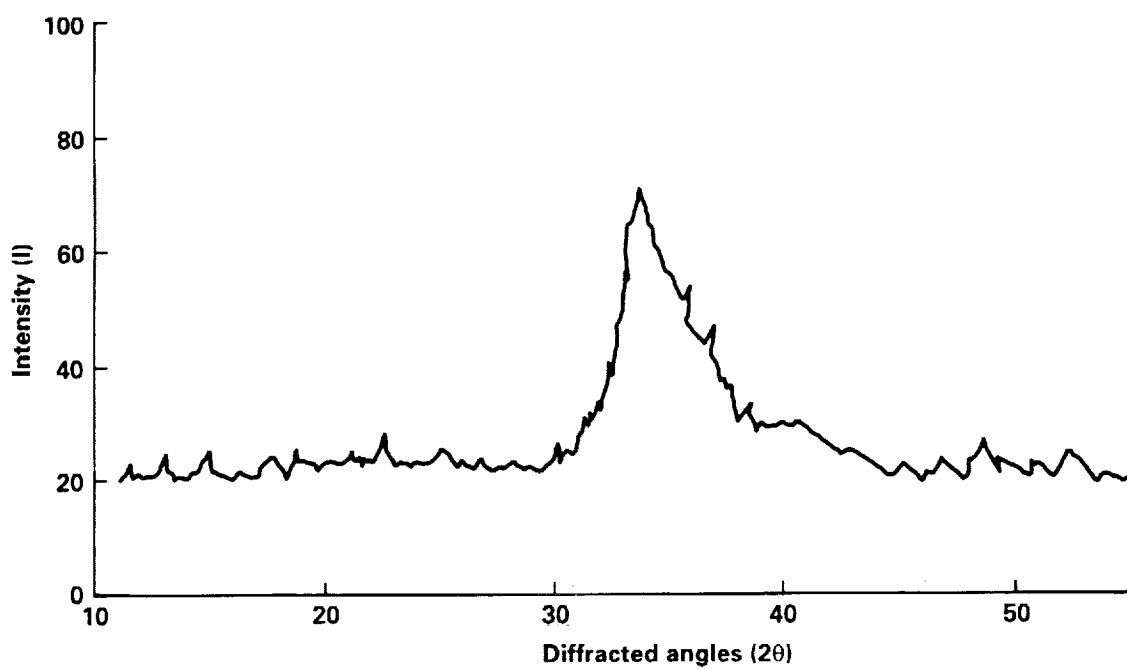


Figure 9. X-ray diffraction analysis of SiC fiber exposed at 1200°C for 10 min.

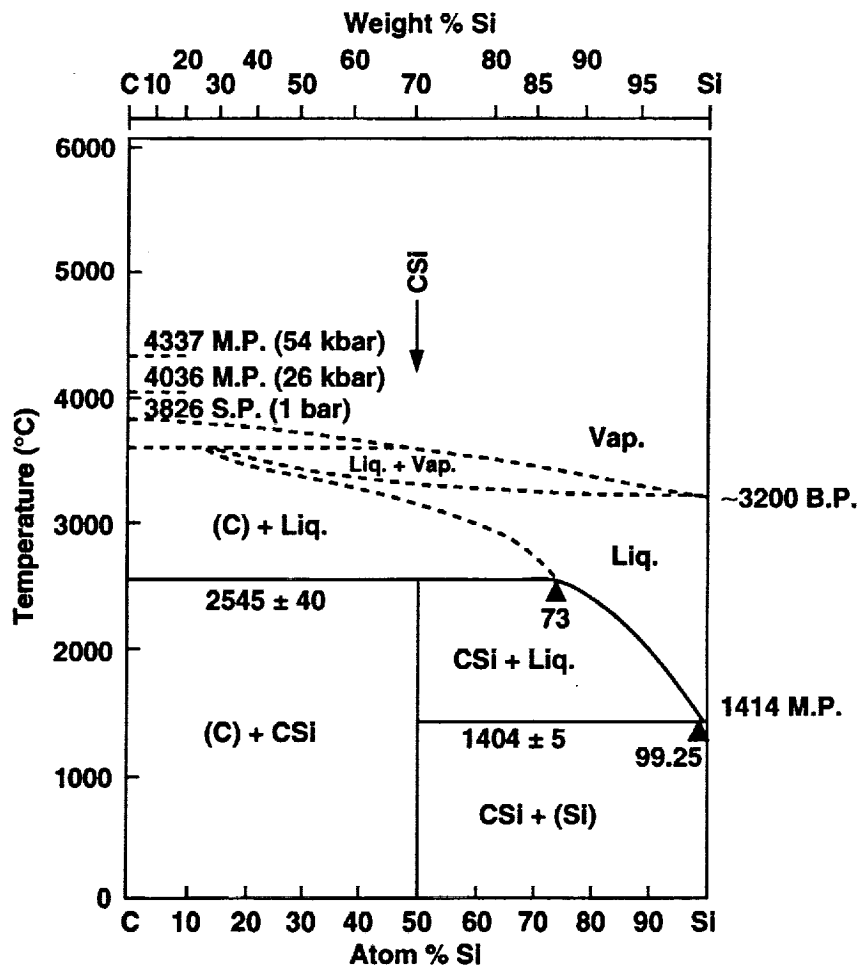


Figure 10. Carbon-silicon phase diagram.

ORIGINAL PAGE
BLACK AND WHITE PHOTOGRAPH



Figure 11. Scanning electron microscopy of non-coated fibers. (a) SiC as-received fiber, (b) SiC fiber exposed at 1200°C for 10 min.

REPORT DOCUMENTATION PAGE

Form Approved
OMB No. 0704-0188

Public reporting burden for this collection of information is estimated to average 1 hour per response, including the time for reviewing instructions, searching existing data sources, gathering and maintaining the data needed, and completing and reviewing the collection of information. Send comments regarding this burden estimate or any other aspect of this collection of information, including suggestions for reducing this burden, to Washington Headquarters Services, Directorate for Information Operations and Reports, 1215 Jefferson Davis Highway, Suite 1204, Arlington, VA 22202-4302, and to the Office of Management and Budget, Paperwork Reduction Project (0704-0188), Washington, DC 20503.

1. AGENCY USE ONLY (Leave blank)		2. REPORT DATE August 1992	3. REPORT TYPE AND DATES COVERED Technical Memorandum	
4. TITLE AND SUBTITLE Thermal Degradation Study of Silicon Carbide Threads Developed for Advanced Flexible Thermal Protection Systems			5. FUNDING NUMBERS 506-43-31	
6. AUTHOR(S) Huy Kim Tran and Paul M. Sawko				
7. PERFORMING ORGANIZATION NAME(S) AND ADDRESS(ES) Ames Research Center Moffett Field, CA 94035-1000			8. PERFORMING ORGANIZATION REPORT NUMBER A-92146	
9. SPONSORING/MONITORING AGENCY NAME(S) AND ADDRESS(ES) National Aeronautics and Space Administration Washington, DC 20546-0001			10. SPONSORING/MONITORING AGENCY REPORT NUMBER NASA TM-103952	
11. SUPPLEMENTARY NOTES Point of Contact: Huy Kim Tran, Ames Research Center, MS 234-1, Moffett Field, CA 94035-1000; (415) 604-0219				
12a. DISTRIBUTION/AVAILABILITY STATEMENT Unclassified — Unlimited Subject Category 27			12b. DISTRIBUTION CODE	
13. ABSTRACT (Maximum 200 words) Silicon carbide (SiC) fiber is a material that may be used in advanced thermal protection systems (TPS) for future aerospace vehicles. SiC fiber's mechanical properties depend greatly on the presence or absence of sizing and its microstructure. In this research, silicon dioxide is found to be present on the surface of the fiber. Electron Spectroscopy for Chemical Analysis (ESCA) and Scanning Electron Microscopy (SEM) show that a thin oxide layer (SiO ₂) exists on the as-received fibers and the oxide thickness increases when the fibers are exposed to high temperature. ESCA also reveals no evidence of Si-C bonding on the fiber surface on both as-received and heat treated fibers. The silicon oxide layer is thought to signal the decomposition of SiC bonds and may be partially responsible for the degradation in the breaking strength observed at temperatures above 400°C. The variation in electrical resistivity of the fibers with increasing temperature indicates a transition to a higher band gap material at 350°C to 600°C. This is consistent with a decomposition of SiC involving silicon oxide formation.				
14. SUBJECT TERMS Silicon carbide, Fiber, Thermoproperty			15. NUMBER OF PAGES 13	
			16. PRICE CODE A02	
17. SECURITY CLASSIFICATION OF REPORT Unclassified	18. SECURITY CLASSIFICATION OF THIS PAGE Unclassified	19. SECURITY CLASSIFICATION OF ABSTRACT	20. LIMITATION OF ABSTRACT	